Origin of Spin Polarization and Magnetic Dichroism in Core-Level Photoemission

B. T. Thole[1] and G. van der Laan[2]

[1]*Materials Science Centre, University of Groningen, 9747 AG Groningen, Netherlands*

[2]*Science and Engineering Research Council Daresbury Laboratory, Warrington WA4 4AD, United Kingdom*

(Received 13 August 1991)

Spin polarization and magnetic circular and linear dichroism in photoemission are interpreted in a many-electron approach. The six different ways to orient the three polarizations in the experiment (magnetization, electric vector of the light, and spin of the photoelectron) allow measurement of six different kinds of correlation between corresponding atomic properties (valence spin, core-hole orbital momentum, and core-hole spin, respectively). This allows us to analyze exchange and hybridization effects and is illustrated for the $2p$ and $3p$ photoemission of ferromagnetic Ni metal.

PACS numbers: 75.25.+z, 75.30.Et, 78.20.Ls, 79.60.Cn

Core-level photoemission (XPS) contains much information on the electronic structure of transition-metal and rare-earth materials. However, the interpretation is not unambiguous in the assignment of structures to either configuration mixing, core-hole interaction, or band structure. According to the Kotani-Toyozawa model [1] the main and satellite peaks in narrow-band metals correspond to a well and a poorly screened core-hole state. But line splittings can also be caused by core-valence exchange or Coulomb interactions [2]. Constraints on the theory are obtained if we treat XPS together with x-ray absorption or Auger spectroscopy in the same model [3], but this requires great care since these spectroscopies have a different number of final-state holes. A more direct way to analyze the structures in XPS is to measure their spin and x-ray polarization dependence.

Spin polarization in valence-band photoemission is a well-known effect. It has been interpreted using band theory, where each electron moves independently in a relativistic potential which includes spin-dependent exchange and spin-orbit interactions. In ferromagnetic $3d$ transition metals the valence band is oriented by exchange interaction, and since the photoelectrons retain their spin orientation during the excitation, their polarization yields the majority and minority spin density of states. In $4d$, $4f$, $5d$, and $5f$ metals the valence band is split by spin-orbit interaction, coupling the orbital momentum to the polarized spin. This makes the emission sensitive to the polarization of the light.

Polarized core-level XPS measurements have started only recently. Spin polarization in the Fe $3s$ and $3p$ core levels [4,5] and magnetic circular dichroism in the Fe $2p$ core-level photoemission of ferromagnetic iron [6] have so far been reported. The large effort currently invested in beam lines and insertion devices for polarized x rays [7] promises a rapid development of this area. However, core-level photoemission in narrow-band materials requires a many-electron approach, taking into account core-valence electrostatic interactions. In this Letter we present such an approach. We show that there are six different ways to correlate the polarization of the spin of the ground state to the orbital momentum and the spin of the excited core electron. We will demonstrate the potentialities of this analysis on the case of ferromagnetic nickel metal.

In a general setup for polarized XPS [8], circularly or linearly polarized light impinges on a magnetically ordered sample and the intensity of the emitted electrons is measured for both up and down spin as a function of energy. We do not consider here the angular distribution or the final-state interactions of the photoelectrons. Thus for some fixed magnetization M of the sample we obtain six spectra $I_{q\sigma}$, where $q=-1$, 0, and 1 for left, Z, and right circularly polarized light and $\sigma=\uparrow$ and $\downarrow$ for spin up and spin down, respectively. Reversal of the magnetization produces no additional spectra because, in an obvious notation, $I_{-q-\sigma-M}=I_{q\sigma M}$.

These six spectra are all more or less different, and for each material we might be satisfied by a theory which reproduces these spectra. However, analysis shows that we can assign specific differences between the spectra to specific physical effects, thus allowing us to draw definite conclusions. This is possible when we take the linear combinations I^{xy} ($x=0,1,2$ and $y=0,1$) defined in Table I. It may be checked that a spectrum with $x=0$ can be measured using isotropic light, and $x=1$ measures circular and $x=2$ linear dichroism. When $y=0$, no spin polarization needs to be measured, while $y=1$ denotes the difference spectrum for spin up and spin down.

The atomic photoemission process is depicted in Fig. 1. It shows a system consisting of a valence shell and a core shell with momenta S_v,L_v and L_c,S_c, respectively. In a localized model there are exchange interactions between S_v and S_c, Coulomb interactions between L_v and L_c, and spin-orbit interactions between L and S of the same shell. The exchange field polarizes the valence spin S_v of the ground state which means that only some of the magnetic sublevels m are populated giving nonisotropic values for $\langle M\rangle$, $\langle M^2\rangle$, $\langle M^3\rangle$, etc. The electric polarization vector q of the light acts on the core orbital momentum L_c, producing polarized core-hole (and photoelectron) orbitals, and the photoelectron spin polarization σ measured is the same as that of the core-hole spin S_c. We indicate the multipole moments x, y, and z of the polarizations by

TABLE I. The six fundamental photoemission spectra I^{xy}, which are linear combinations of the primitive spin-polarized spectra. $x=0,1,2$ denotes isotropically, circularly, and linearly polarized radiation, respectively. $y=0,1$ denotes without and with spin-polarization measurement, respectively. In the column labeled z, a value 1, 2, or 3 denotes that $\langle M\rangle$, $\langle M^2-\frac{1}{3}J(J+1)\rangle$, or $\langle M^3-\frac{3}{5}M[J(J+1)-\frac{1}{3}]\rangle$ in the ground state has to be nonzero to obtain the spectrum; $z=0$ denotes the value of the monopole, which is always unity.

I^{xy}	Combination of primitive spectra	z	Significance
I^{00}	$I_{1\uparrow}+I_{0\uparrow}+I_{-1\uparrow}+I_{1\downarrow}+I_{0\downarrow}+I_{-1\downarrow}$	0	Isotropic spectrum
I^{01}	$I_{1\uparrow}+I_{0\uparrow}+I_{-1\uparrow}-I_{1\downarrow}-I_{0\downarrow}-I_{-1\downarrow}$	1	Spin spectrum
I^{10}	$I_{1\uparrow}-I_{-1\uparrow}+I_{1\downarrow}-I_{-1\downarrow}$	1	Orbit spectrum (MCD)
I^{11}	$I_{1\uparrow}-I_{-1\uparrow}-I_{1\downarrow}+I_{-1\downarrow}$	0,2	Spin-orbit spectrum
I^{20}	$I_{1\uparrow}-2I_{0\uparrow}+I_{-1\uparrow}+I_{1\downarrow}-2I_{0\downarrow}+I_{-1\downarrow}$	2	Anisotropic spectrum (MLD)
I^{21}	$I_{1\uparrow}-2I_{0\uparrow}+I_{-1\uparrow}-I_{1\downarrow}+2I_{0\downarrow}-I_{-1\downarrow}$	1,3	Anisotropic spin magnetic spectrum

0,1,2,3 for isotropic, dipole, quadrupole, and octupole moments, respectively. For a spectrum to be observable, interactions connecting the nonzero values of x, y, and z in Fig. 1 are required.

The physical picture in Fig. 1 can be formulated in an exact way. It can be shown that a spectrum I^{xy} is nonzero when a zth moment has been induced in the atoms of the sample by the exchange field, where z must be in the range $|x-y|,\ldots,(x+y)$ and $x+y+z$ is even. When this is the case, the spectrum measures the amount of correlation (alignment) of the xth moment of the orbital momentum of the core hole with the yth moment of the core-hole spin and the zth moment induced in the ground state. This correlation is different for each final state; thus we obtain information on the character of each final state. Moreover, when such a correlation between moments is observed, this indicates the presence and effects of the specific interactions that cause this correlation.

The first fundamental spectrum I^{00} is the familiar isotropic spectrum. It measures the parentage of the ground state to the final states. This Letter mainly analyzes those polarized spectra where one of the x,y,z is zero and the other two are 1. For qualitative purposes we can say that the spectrum $I^{01}(z=1)$ measures S_cS_v, i.e., the alignment of the core-hole spin with the valence spin. Likewise, $I^{10}(z=1)$ measures $-L_cS_v$, and $I^{11}(z=0)$ measures $-L_cS_c$, the core-hole spin-orbit coupling.

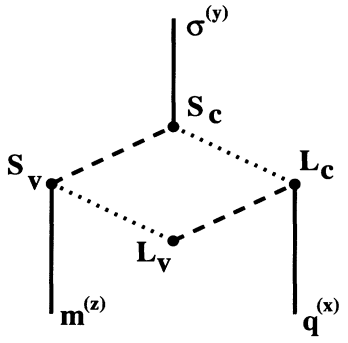

FIG. 1. Schematic picture for spin-polarized photoemission with spin-orbit interactions (dotted lines) and electrostatic interactions (dashed lines). $L_{v(c)}$ and $S_{v(c)}$ denote the orbital and spin moments of the valence (core) state, respectively; x, y, and z are the polarizations of the electric vector q, the spin σ, and the magnetic moment m. For a polarization spectrum to be observable we need interactions connecting the nonzero values of x, y, and z.

In I^{01}, the electric vector q is isotropic ($x=0$) and cannot produce polarized core-hole orbitals, but the sample has a magnetic moment ($z=1$) and we measure the spin polarization ($y=1$). To couple the m and σ polarization requires at least exchange interaction between S_v and S_c. The exchange interaction directly couples the spins of the core hole and valence holes; neither spin-orbit coupling nor circular polarization is needed to polarize the core-hole spin and thus the photoelectron spin.

In I^{10} (magnetic circular dichroism) no spin polarization is measured ($y=0$), but m is polarized ($z=1$) and the difference in total emission for right and left circular polarization is measured ($x=1$). The required coupling between L_c and S_v is always indirect: The photon spin creates a core hole with polarized orbital momentum, which is coupled by the electrostatic and spin-orbit interaction to the spin of the valence electrons [9]. Figure 1 shows that there are two possible ways to do this.

The I^{11} spectrum has two z contributions: 0 and 2. It is clear from Fig. 1 that in the $z=0$ contribution, core-hole spin-orbit interaction is required, but no interaction with the valence electrons is needed. The photon spin acts on (polarizes) the electron spin via the spin-orbit coupling. Since no interaction is needed between the core and valence levels this spectrum can also be obtained in nonmagnetic atoms or in the one-electron model.

The cases in which x, y, or z are larger than 1 are too complicated to allow a simple explanation of the behavior of each peak in the spectrum. We will only discuss the conditions under which these spectra are nonzero.

The I^{20} spectrum measures the difference in emission using perpendicular and parallel linearly polarized light ($x=2$), hence magnetic linear dichroism. The spin is not

detected. Since $z=2$ (quadrupole polarization), this spectrum is present in both ferromagnets and antiferromagnets, where $\langle M\rangle=0$, but $\langle M^2\rangle - J(J+1)/3 \neq 0$, when J or $S > \frac{1}{2}$. In the latter case it measures a many-electron effect. A quadrupole can also be induced by a low-symmetry crystal field (keeps M and $-M$ degenerate). The crystal field polarizes L_v and of course this moment couples in a specific way to the other moments. The importance of this spectrum is that it is relatively simple to measure.

Finally, in the I^{21} spectrum we need a magnetic dipole or octupole moment to measure spin polarization using linearly polarized light. Spin-orbit as well as Coulomb interactions are needed. In theory, the $z=1$ and 3 contributions can be determined separately when we vary the magnetic polarization, e.g., by temperature dependence, giving information on the effects of both $\langle M\rangle$ and $\langle M^3\rangle$.

We will now demonstrate the theory on the $2p$ and $3p$ XPS spectra of ferromagnetic Ni metal. Figures 2 and 3 show the primitive spectra for emission to d continuum states. The fundamental spectra shown are those for emission to the s continuum, which are stronger by a factor of 1, -2, and 10 than those for d emission for $x=0$, 1, and 2, respectively. The spectra were calculated using an Anderson impurity model [10]. A ground state consisting of a mixture of d^8, d^9, and d^{10} with weights of 8%, 44%, and 48%, respectively [11], gives a good agreement with the experimental $2p$ and $3p$ isotropic XPS [12] and magnetic x-ray dichroism (MXD) in x-ray absorption [13,14].

In $2p$ XPS (Fig. 2), the most pronounced spectrum is I^{11}. This measures I^{00} times $-L_cS_c$, which is $\frac{1}{2}$ in $p_{3/2}$ and -1 in $p_{1/2}$. In the presence of core-valence exchange interactions (not in p^5d^{10}), I^{11} is not such a trivial copy of I^{00}. Deviations are not visible in Fig. 2(b), but are present in other cases [8]. However, exchange effects manifest themselves most directly in I^{01}, where high-spin final states (S_vS_c positive) give positive peaks and low-spin states give negative peaks. Two typical Hund's rule effects can be observed in the p^5d^9 peaks. First, $p_{3/2}$ states are mixed with $p_{1/2}$ states giving a surplus of high spin in the $p_{3/2}$ edge and low spin in $p_{1/2}$. Second, within the $p_{3/2}$ edge, there is more high spin at the low-energy side and low spin at the high-energy side. This effect is practically absent in $p_{1/2}$ because the exchange interactions of the valence electrons with $p_{1/2}$ are weak [15]. The $p_{3/2}d^{10}$ peak is positive, because it mixes most strongly with the nearby high-spin part of $p_{3/2}d^9$. The I^{10} spectrum shows $-L_cS_v$. The polarization of L_c is produced indirectly. First, S_c is polarized by exchange interactions with S_v, producing I^{01}. Then, by core-hole spin-orbit coupling, L_c is aligned parallel or antiparallel to S_c in $p_{3/2}$ and $p_{1/2}$, respectively. This second step makes I^{10} very similar to I^{01} apart from the sign change between the two edges (but I^{10} is more easy to measure). Again, the similarity of these spectra is less for other configurations. In the $3p$ XPS (Fig. 3), the core spin-orbit coupling is no longer dominating and core-valence Coulomb interactions come to the front. The spin spectrum I^{01} clearly shows a negative low-spin $^1P\,^1F$ and positive high-spin $^3P\,^3D$ peak. In the I^{10} spectrum, the alignment of L_c with S_v is again produced indirectly but now mainly via the other route in Fig. 1. By valence spin-orbit coupling, L_v is antiparallel to S_v. Next, core-valence Coulomb interactions couple L_c to L_v; in the F, D, and P states they are parallel, weakly, and strongly antiparallel, respectively. In the $^1P\,^1F$ peak, the effects of P and F almost cancel; in the $^3P\,^3D$ peak, the ^3P gives the net parallel alignment of L_c and S_v; and in the low-energy structure, ^3F gives the net antiparallel peak. This

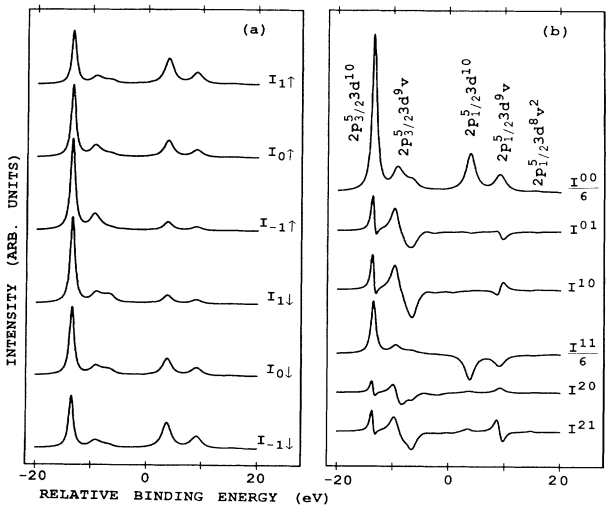

FIG. 2. Ni $2p$ spin-polarized photoemission of Ni metal, (a) primitive and (b) fundamental spectra.

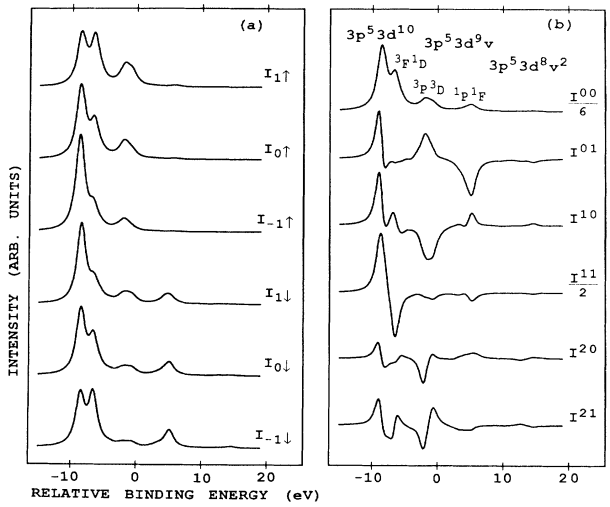

FIG. 3. Ni $3p$ spin-polarized photoemission of Ni metal, (a) primitive and (b) fundamental spectra.

indirect coupling gives a net alignment of S_c and L_c even in the absence of core spin-orbit interaction, giving the effect that I^{11} is to some extent a product of I^{01} and I^{10}. But the *real* spin-orbit interaction in p^5d^{10}, which has no Coulomb interactions, is more effective, giving the dispersive curve at the low-energy side.

In conclusion, polarized photoemission of core levels in transition-metal, rare-earth, and actinide magnetic systems greatly increases the amount of information on the magnetic moment of the ground state and on the interaction of this moment with the spin and orbit of the hole created. The analysis presented can also be used to choose the best strategy to measure specific physical effects.

[1] A. Kotani and Y. Toyozawa, J. Phys. Soc. Jpn. **37**, 912 (1974).

[2] D. A. Shirley, in *Photoemission in Solids I,* edited by M. Cardona and L. Ley (Springer-Verlag, Berlin, 1978), p. 167.

[3] L. C. Davis, J. Appl. Phys. **59**, R25 (1986).

[4] C. Carbone and E. Kisker, Solid State Commun. **65**, 1107 (1988); C. Carbone, T. Kachel, R. Rochow, and W. Gudat, Z. Phys. B **79**, 325 (1990); Solid State Commun. **77**, 619 (1991).

[5] F. U. Hillebrecht, R. Jungblut, and E. Kisker, Phys. Rev. Lett. **65**, 2450 (1990).

[6] L. Baumgarten, C. M. Schneider, H. Petersen, F. Schäfers, and J. Kirschner, Phys. Rev. Lett. **65**, 492 (1990).

[7] Synchrotron Radiation Instrumentation Conference Proceedings, Chester, 1991 [Rev. Sci. Instrum. (to be published)].

[8] B. T. Thole and G. van der Laan, Phys. Rev. B (to be published).

[9] G. van der Laan, Phys. Rev. Lett. **66**, 2527 (1991).

[10] Details of the calculational method are given in Ref. [8].

[11] For Ni metal we used as parameters $E(d^{10})=0$, $E(d^9)=0.75$, $E(d^8)=3.75$, $Q(2p,3d)=Q(3p,3d)=4.25$, $V_{\text{mixing}}(SO_3)=0.7$, $V_{\text{mol.field}}=0.5$ eV. (Recently, T. Jo and G. A. Sawatzky [Phys. Rev. B **43**, 8771 (1991)] used a different parameter set to calculate the $2p$ MXD. However, for XPS these parameters result in satellites that are too high.) The Slater (reduced to 80%) and spin-orbit parameters were given by G. van der Laan and B. T. Thole [Phys. Rev. B **43**, 13401 (1991)]. Lorentzian linewidths: $\Gamma(2p)=1$ (0.5 for first peak); $\Gamma(3p)=0.8$ eV.

[12] S. Hüfner and G. K. Wertheim, Phys. Lett. **51A**, 299 (1975).

[13] C. T. Chen, F. Sette, Y. Ma, and S. Modesti, Phys. Rev. B **42**, 7262 (1990).

[14] T. Koide *et al.* Phys. Rev. B **44**, 4697 (1991).

[15] K. Okada, A. Kotani, and B. T. Thole (unpublished).